q dependence of the dynamic susceptibility $\chi''(\mathbf{q},\omega)$ in superconducting $YBa_2Cu_3O_{6.6}$ ($T_c = 46$ K)

B. J. Sternlieb, J. M. Tranquada, and G. Shirane
Department of Physics, Brookhaven National Laboratory, Upton, New York, 11973

M. Sato and S. Shamoto
Department of Physics, Nagoya University, Nagoya, 464-01, Japan
(Received 15 April 1994)

q-dependent neutron-scattering measurements of the dynamic susceptibility $\chi''(\mathbf{q},\omega)$ in superconducting $YBa_2Cu_3O_{6.6}$ are presented. The observed magnetic scattering near the antiferromagnetic zone center has a nontrivial, approximately flat-topped **q** dependence. A separable model of the susceptibility, $\chi''(\mathbf{q},\omega)=\chi''(\omega)F(\mathbf{q})$, is found to describe this scattering at all energies in the range 2 meV $\leq\hbar\omega\leq$ 40 meV. Measurements at temperatures above and below $T_c = 46$ K indicate that the **q**-dependent "shape" function, $F(\mathbf{q})$, is the same in both the superconducting and normal states. A phenomenological expression for $F(\mathbf{q})$ is presented and the physical significance of its parametrization is discussed. These results are compared with current theories in the literature.

I. INTRODUCTION

The ubiquitous presence of antiferromagnetic spin fluctuations in the high-T_c cuprates has generated a great deal of interest in the role played by magnetism in these compounds. Inelastic neutron-scattering measurements, which directly measure the energy and **q** dependence of the imaginary part of the dynamic spin susceptibility, $\chi''(\mathbf{q},\omega)$, have been particularly useful in determining which features of $\chi''(\mathbf{q},\omega)$ are shared by these materials and which are particular to a given chemical composition. Comparison of these similarities and differences, particularly in $La_{1.85}Sr_{0.15}CuO_4$ and "underdoped" $YBa_2Cu_3O_{6+x}$, has placed strong constraints on theories describing these oxides.

The energy dependence of $\chi''(\mathbf{q},\omega)$ at low temperatures exemplifies the similar magnetic character of these cuprates. In both superconducting $La_{1.85}Sr_{0.15}CuO_4$ (Refs. 1 and 2) and $YBa_2Cu_3O_{6+x}$,[3,4] the $2d$ integrated susceptibility, $\chi''_{2d}(\omega)\equiv\int d^2q\chi''(\mathbf{q},\omega)$, is strongly suppressed at low energies. This reduction is accompanied, at higher energies, by an enhancement of $\chi''_{2d}(\omega)$ relative to the susceptibilities measured in the undoped antiferromagnetic compounds La_2CuO_4 and $YBa_2Cu_3O_6$.[5]

In contrast, the **q** dependences of $\chi''(\mathbf{q},\omega)$ observed in these materials are surprisingly different. In $La_{1.85}Sr_{0.15}CuO_4$, the magnetic scattering is incommensurate with the underlying crystal lattice, with four, sharp rods of scattering symmetrically located about the $2d$ antiferromagnetic zone center at $(\frac{1}{2}\pm\delta,\frac{1}{2},l)$ and $(\frac{1}{2},\frac{1}{2}\pm\delta,l)$.[6,7] The width of the scattering from these $2d$ rods is observed to increase with increasing energy and more weakly, with increasing temperature.[1,8] In $YBa_2Cu_3O_{6+x}$, the magnetic scattering is broadly peaked about the antiferromagnetic zone center, with an overall width comparable to the incommensurate splitting observed in $La_{1.85}Sr_{0.15}CuO_4$. A number of experiments have suggested that the temperature and energy dependence of the width of this scattering is very weak.[4,9]

Previous neutron studies of $YBa_2Cu_3O_{6+x}$ have largely used a single Gaussian to model the **q** dependence of $\chi''(\mathbf{q},\omega)$. However, work by Tranquada *et al.* on a $T_c = 53$ K, $YBa_2Cu_3O_{6.6}$ crystal (labeled #30b) has shown, at an energy transfer of $\Delta E = 15$ meV, that the magnetic scattering has more of a flat-topped shape. The nontrivial **q** dependence of this data, and recent theoretical interest in the evolution of the **q** dependence of $\chi''(\mathbf{q},\omega)$ with changing temperature and energy, have motivated a more in-depth study of the dynamic susceptibility in $YBa_2Cu_3O_{6+x}$.

In this paper we present detailed measurements of the **q** dependence of $\chi''(\mathbf{q},\omega)$ in superconducting $YBa_2Cu_3O_{6.6}$. Measurements were performed at a number of transfer energies between $\Delta E = 2$ meV and $\Delta E = 40$ meV at temperatures $T = 10$ K ($< T_c$) and $T = 60$ K ($> T_c$). Our results demonstrate that the dynamic susceptibility can be written as the separable product of energy- and momentum-dependent terms, $\chi''(\mathbf{q},\omega)=\chi''(\omega)F(\mathbf{q})$ in this temperature and energy range. A phenomenological shape function, $F(\mathbf{q})$, is presented and the physical significance of its parametrization is discussed. Results demonstrating the identical character of $F(\mathbf{q})$ in the normal and superconducting states are also presented. We conclude with a comparison of our results with outstanding theories in the literature.

II. EXPERIMENTAL DETAILS

The crystal used for these measurements, labeled #46, was grown at Nagoya University. It has a 1.2° mosaic and a volume of ~ 1 cm^3.[10] Ac susceptibility measurements indicate a superconducting transition temperature of $T_c = 46$ K. Lattice constants measured on a calibrated spectrometer at room temperature are $a = 3.840$ Å, $b = 3.878$ Å, and $c = 11.727$ Å.

The measurements were performed on the H8 triple-axis spectrometer at Brookhaven National Laboratory's High Flux Beam Reactor. The (002) reflection of pyro-

lytic graphite was used to monochromate and analyze the incident and scattered beams. Except where noted, measurements were done using a 40'-40'-*S*-80'-80' horizontal and 60'-75'-*S*-190'-420' vertical collimation configuration and a fixed final energy, $E_f = 14.7$ meV. A pyrolytic graphite filter was used to remove higher-order (λ/n) contamination from the scattered beam. The crystal was mounted on the cold finger of a Displex helium refrigerator in an aluminum can backfilled with helium exchange gas. The sample was oriented with the $[1\bar{1}0]$ axis normal to the scattering plane to allow the study of momentum transfers $\mathbf{q} \in (h,h,l)$.

The magnetic fluctuations in superconducting $YBa_2Cu_3O_{6+x}$ are predominantly $2d$ in character. However, the finite coupling between CuO_2 bilayers results in a sinusoidal modulation of the scattering intensity, $\mathcal{I}(\mathbf{q},\omega)$, with momentum transfers normal to the CuO_2 planes:[4]

$$\mathcal{I}(\mathbf{q},\omega) \sim [n(\omega)+1][\chi''(\mathbf{q},\omega)\cdot\sin^2(\pi l z)] \ .$$

Here $n(\omega)$ is the Bose occupation function and $z\cdot c = 3.342$ Å is the distance between adjacent copper-oxide planes. With the $\sin^2(\ )$ modulation term explicitly factored, $\chi''(\mathbf{q},\omega)$ is only weakly dependent on momentum transfers parallel to the reciprocal-lattice vector c^*. As the modulation along c^* is both energy and temperature independent, most of our data were taken at $l = -1.8$ to maximize the measured scattering intensity. Measurements at $\Delta E = 30$ and 40 meV required larger momentum transfers, $l = -5.4$, to close the spectrometer scattering triangle.[11]

III. EXPERIMENTAL RESULTS

In Fig. 1 we show the scattering intensity measured at $T = 10$ K along $\mathbf{q} = (h,h,-1.8)$ at constant energy transfers of $\Delta E = 6$, 9, 12, 15, and 18 meV and along $\mathbf{q} = (h,h,-5.4)$ at $\Delta E = 30$ meV. The weak intensities observed at $\Delta E = 6$ meV, and to a lesser extent, $\Delta E = 9$ meV, reflect the suppression of the low-energy scattering at low temperatures due to the $\Delta_{SG} \approx 6$-meV spin "pseudogap" in this crystal.[4,9] The effect of this gap on the energy dependence of χ'' at $T = 10$ K is shown, with comparable data from a similar crystal (#30b $T_c = 53$ K),[9] in Fig. 2. Here we concentrate on the q-dependent shape of the observed magnetic scattering. The $\Delta E = 12$, 15, and 18 meV spectra of Fig. 1 evince the same flat-topped form first observed by Tranquada *et al.*[4] At $\Delta E = 30$ and 40 (not shown) meV, the data appear more rounded. However, this dependence of the line shape on energy is largely an artifact of the energy dependence of the spectrometer resolution. The full width at half maximum (FWHM) q-space extent of this resolution along the zone diagonal (scan direction) is shown for each energy in Fig. 1. To determine whether variations in the q dependence of $\chi''(\mathbf{q},\omega)$ with energy can be *entirely* attributed to instrumental effects, a separable expression for the dynamic susceptibility,

$$\chi''(\mathbf{q},\omega) = \chi''(\omega)\cdot F(\mathbf{q}) \qquad (1)$$

was convoluted with the spectrometer resolution to fit

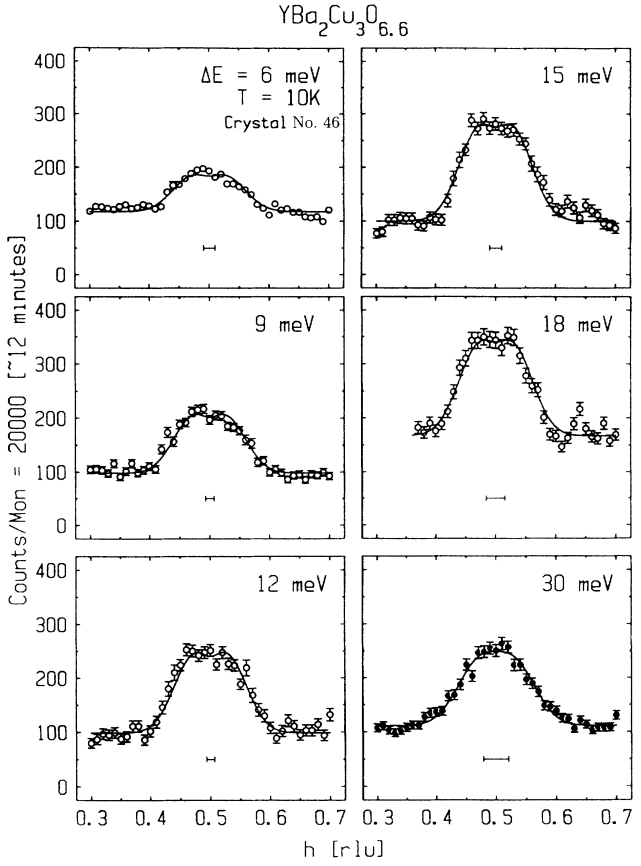

FIG. 1. Constant energy scans at $T = 10$ K along $\{(h,h,l)|\circ: l = -1.8, \bullet: l = -5.4\}$. The solid lines are fits to the data using a constant, energy-independent shape function, $F(\mathbf{q})$. The spectrometer resolution at each energy along the scan direction is also shown.

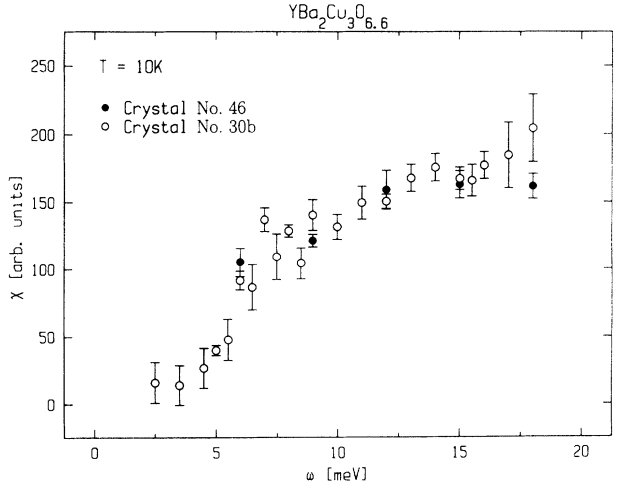

FIG. 2. $\chi''(\omega)$ vs ω at 10 K. (●): Amplitudes from Fig. 1. (○): Results of peak intensity measurements on a similar crystal (Ref. 9).

these measurements.[12] As shown by the solid curves through the data, a global fit to this product of a single, energy-independent shape function, $F(\mathbf{q})$, and an energy-dependent amplitude, $\chi''(\omega)$, results in a surprisingly good fit, $\chi^2_{\text{global}}=1.73$. The quality of this fit indicates that the $\mathbf{q}$ dependence of our data is, within error, independent of energy.

The phenomenological shape function used in these fits,

$$F(\mathbf{q})=e^{-\ln 2\cdot(|\mathbf{q}|-\beta)^2/(\alpha-\beta)^2}, \tag{2}$$

provides a convenient parametrization of the half width at half maximum (HWHM) extent of the scattering, α, and a measure of the offset, β, of the peak in $\chi''(\mathbf{q},\omega)$ from the zone corner, $(\frac{1}{2},\frac{1}{2},l)$. For the global fit shown in Fig. 1, these parameters are $\alpha=0.155(3)$ Å^{-1} and $\beta=0.067(4)$ Å^{-1}. In Fig. 3, we graph Eq. (2) using these fit values for α and β. Though the form of this function has no *a priori* physical justification, the nontrivial $\mathbf{q}$ dependence of $F(\mathbf{q})$ suggests two distinct possibilities for the underlying scattering: (1) the scattering is single component, albeit with a complex line shape; or (2) the scattering is the sum of incommensurate contributions as shown, for instance, in the inset to Fig. 3.

In the first case, Eq. (2) provides a much better fit to the data than conventional Gaussian or Lorentzian-squared line shapes. This is illustrated by fits of the $\Delta E=15$-meV data to these line shapes, shown in Fig. 4, which demonstrate that Eq. (2) better accounts for both the flat-topped character of $\chi''(\mathbf{q},\omega)$ near $(\frac{1}{2},\frac{1}{2},-1.8)$ and the absence of Lorentzian-like "tails" in the measured spectra. The HWHM $\mathbf{q}$ widths that characterize this scattering are strongly dependent on the choice of shape function. As discussed below, this dependence is particularly important to the proper analysis of NMR spin-relaxation data on these systems. These HWHM values

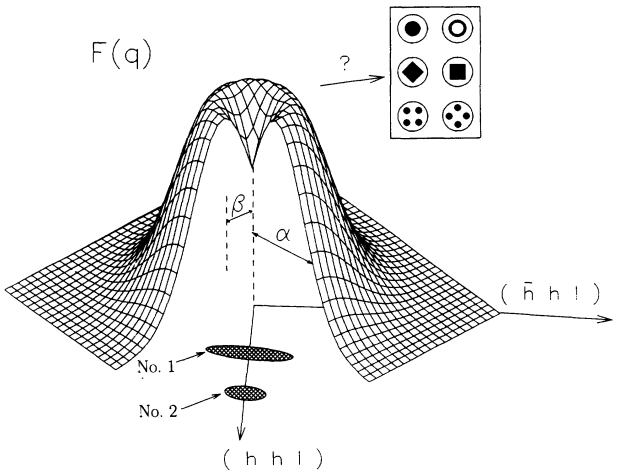

FIG. 3. The shape function $F(\mathbf{q})$ drawn with the global fit parameters, $\alpha=0.155(3)$ Å^{-1} and $\beta=0.067(4)$ Å^{-1}, from the data of Fig. 1. (#1): Spectrometer resolution with 60'-75'-*S*-190'-420' and (#2): 60'-75'-*S*-190'-40' vertical collimation. (inset) Some possible geometries for the underlying structure of $F(\mathbf{q})$.

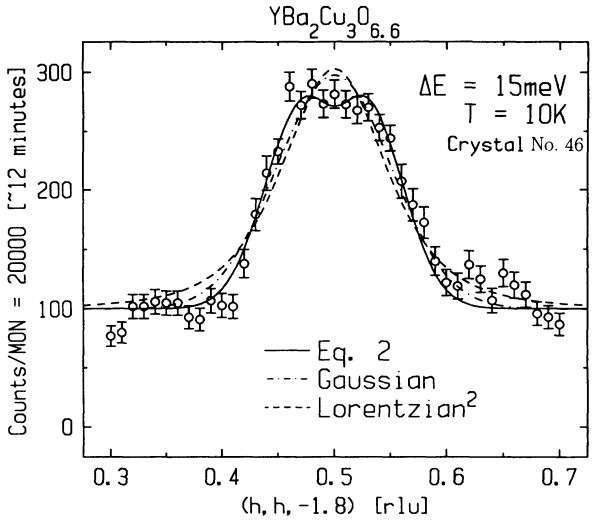

FIG. 4. $T=10$ K, $\Delta E=15$-meV data fit with Eq. (2), a Gaussian, and a Lorentzian-squared line shape. Equation (2) better models the central flat-topped character and sharp falloff with q of the observed scattering.

and the parameters from these fits are summarized in Table I.

Investigation of the latter possibility, that the scattering is the sum of multiple components, is hindered by finite spectrometer resolution. This is illustrated in Fig. 3 which shows the FWHM projection of the spectrometer resolution ellipsoid, labeled #1, corresponding to the measurement configuration used in the 15-meV scan of Fig. 4. The relatively large width along the major axis of this ellipse, FWHM$=0.146$ Å$^{-1}\sim 2\times\beta$, which is due to the relaxed vertical collimation used in these measurements, tends to average over any variations in the detailed structure of $F(\mathbf{q})$ such as those shown in the inset to Fig. 3. Efforts to better characterize $F(\mathbf{q})$ were made by tightening the resolution with a 60'-75'-*S*-190'-40' vertical collimation configuration as shown in Fig. 3, #2. However, as shown in Fig. 5, the resulting data are readily fit using Eq. (2) and do not offer any additional constraint to the underlying form of $F(\mathbf{q})$. Unfortunately, the benefits of further reducing the resolution volume are limited by a concommitant drop in scattering intensity.

Representative normal state, $T=60$ K, data at $\Delta E=2$, 18, and 30 meV are shown in Fig. 6. To reduce background, the 2-meV data were taken using a fixed incident

TABLE I. χ^2 and fit parameters from the data in Fig. 4. The resulting HWHM $\mathbf{q}$ width of the scattering is highly dependent on the choice of fit function.

$F(\mathbf{q})$	χ^2	parameters (rlu)	HWHM (Å^{-1})
Eq. (2)	1.8	$\alpha=0.068(2)$ $\beta=0.031(3)$	0.156(5)
$e^{-\ln 2q^2/\kappa_g^2}$	2.5	$\kappa_g=0.059(3)$	0.136(7)
$\frac{1}{(\kappa_l^2+q^2)^2}$	3.4	$\kappa_l=0.080(6)$	0.118(8)

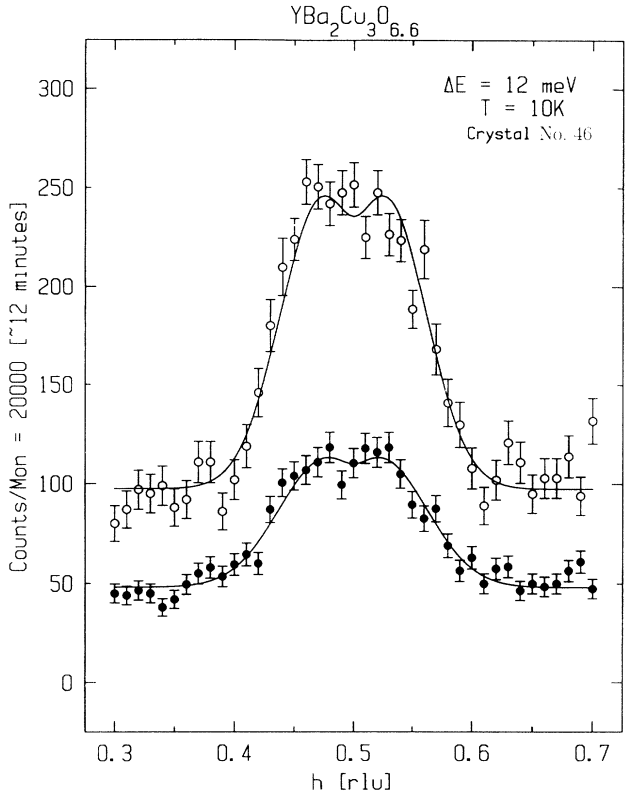

FIG. 5. $\Delta E = 12$-meV measurements with (○): 60'-75'-S-190'-420' and (●): 60'-75'-S-190'-40' vertical collimation. The higher-resolution data do not reveal any additional features in $F(\mathbf{q})$.

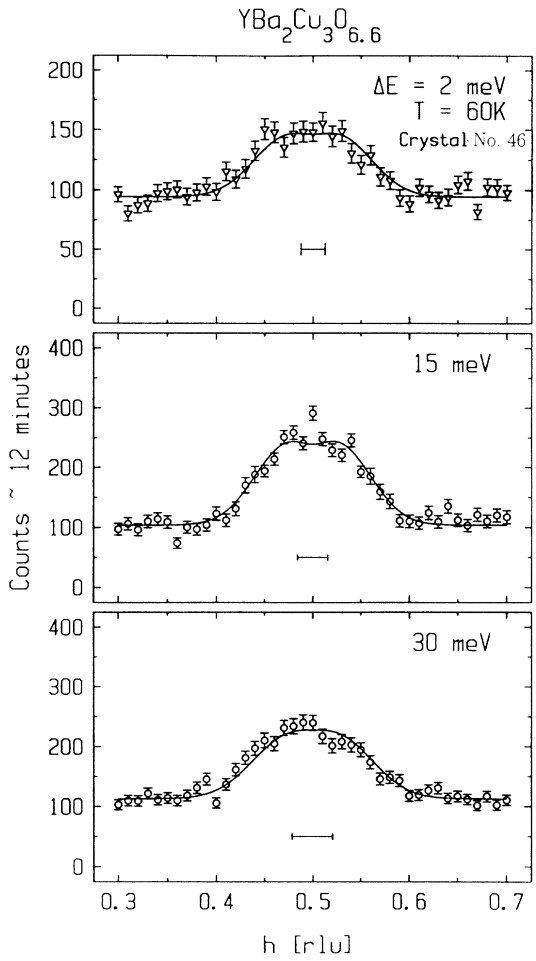

FIG. 6. Constant energy scans at $T = 60$ K. Solid lines are fits using the same parametrization of $F(\mathbf{q})$ as used in the 10-K data of Fig. 1.

energy, $E_i = 14.7$ meV, spectrometer configuration. These data clearly have a $\mathbf{q}$ dependence similar to that observed in the $T = 10$-K data of Fig. 1. A global fit to these spectra and additional data at $\Delta E = 6$, 9, 12, and 15 meV result in parameters for Eq. (2), $\alpha = 0.151(4)$ Å^{-1} and $\beta = 0.062(6)$ Å^{-1}, that are in good agreement with the 10-K values. This result suggests that the shape function $F(\mathbf{q})$ is unaffected by the superconducting transition at $T_c = 46$ K. We note that this normal/superconducting state similarity occurs for energy transfers both above and below the spin pseudogap.

IV. CONCLUSION

Our measurements extend the preliminary shape results of Tranquada *et al.*[4] and demonstrate that the $\mathbf{q}$ dependence of $\chi'(\mathbf{q},\omega)$ has nontrivial structure for all energies 2 meV $< \Delta E <$ 40 meV. Our principal conclusion is that this $\mathbf{q}$ dependence is *independent* of energy in this range. We stress that this independence contrasts with the energy variation of $F(\mathbf{q})$ observed in superconducing $La_{1.85}Sr_{0.15}CuO_4$.[1,8] In addition, measurements at $T = 10$ K and $T = 60$ K show that the same parametrization of Eq. (2), or the same shape function, can be used to fit data in both the superconducting and normal states. The underlying symmetry and detailed structure of $F(\mathbf{q})$ remain open questions. The relatively tight vertical resolution data of Fig. 5 indicate that any additional features in the $\mathbf{q}$ dependence of $\chi''(\mathbf{q},\omega)$, if present, are quite subtle.

These observations strongly constrain theories of the underdoped cuprates. For instance, in contrast to the observed energy independence of $F(\mathbf{q})$ presented in this paper, the $\mathbf{q}$ width of the phenomenological Millis, Monien, and Pines susceptibility,[13]

$$\chi(\mathbf{q},\omega) = \frac{\chi_Q}{1 + q^2\xi^2 - i(\omega/\omega_{SF})} ,$$

is strongly dependent on energy at frequencies comparable to the characteristic spin-fluctuation energy, ω_{SF}. As the fits presented in Fig. 4 and Table I demonstrate, the Lorentzian-squared line shape resulting from this model, which is commonly used to analyze NMR data,[13,14] also fails to describe the $\mathbf{q}$ dependence of our neutron-scattering results. Barzykin *et al.*[15] have found that the explicit addition of a gap to this expression,

$$\chi(\mathbf{q},\omega) = \frac{\chi_Q}{1 + q^2\xi^2 - \omega^2/\Delta^2 - i(\omega/\omega_{SF})} ,$$

both models the observed spin pseudogap and results in a

mildly incommensurate $\mathbf{q}$ dependence similar to the flat-topped character of our data. However, as noted by the authors,[16] this model requires that the offset of the peak in $\chi''(\mathbf{q},\omega)$ from $\mathbf{q}=(\frac{1}{2},\frac{1}{2},l)$ have an energy dependence of the form

$$\beta=\sqrt{(\omega^2-\Delta^2)/c}$$

when $\omega \gtrsim \Delta$. For plausible values of the gap, Δ, and "velocity," $c \sim \xi \cdot \Delta$, this equation would result in a dramatic energy dependence of $F(\mathbf{q})$ which we clearly do not observe.

We note that recent calculations by Millis and Monien[14] show that the use of a Gaussian line shape, which falls rapidly with $\mathbf{q}$, in preference to a Lorentzian-squared line shape, leads to better agreement with observed O^{17}/Cu^{63} NMR relaxation rates. This conclusion is supported by our data, which are more readily fit with a Gaussian than a Lorentzian-squared line shape as shown in Table I. We believe that a similar calculation employing Eq. (2) might further clarify the NMR results.

Emery and Kivelson[17] have suggested that frustrated phase separation might be responsible for superconductivity in the cuprates. In their model, the behavior of $\chi''(\mathbf{q},\omega)$ is produced by fluctuations of hole-poor magnetic regions induced by interactions with mobile holes. In particular, they argue that the susceptibility can be written [Eq. (4), Ref. 17] as a separable product of terms in which the $\mathbf{q}$ dependence, which is governed by the antiferromagnetic cluster size, is independent of energy and temperature. The agreement of this result with both the form of Eq. (1) and the identity of $F(\mathbf{q})$ in the superconducting and normal states indicates that electronic phase separation may well be important in these systems.

Experiments are currently underway to determine the overall symmetry of $\chi''(\mathbf{q},\omega)$ in $YBa_2Cu_3O_{6+x}$. Comparison with the fourfold, $(\frac{1}{2}\pm\delta,\frac{1}{2},l)/(\frac{1}{2},\frac{1}{2}\pm\delta,l)$ scattering symmetry observed in $La_{1.85}Sr_{0.15}CuO_4$ should clarify the nature of the mechanism responsible for the magnetic response of these materials. An experimentally more difficult question is the characterization of the underlying, possibly incommensurate, structure of $F(\mathbf{q})$ in $YBa_2Cu_3O_{6+x}$. Though efforts to address this issue have proven unsuccessful in the crystal examined in this paper, similar measurements on $YBa_2Cu_3O_{6+x}$ samples with different oxygenation levels may shed more light on this matter.

ACKNOWLEDGMENTS

We wish to thank V. J. Emery and K. Kakurai for discussions regarding our measurements and analysis. Invaluable technical assistance was provided by R. Rothe, J. Biancarosa, and R. J. Liegel. This study was supported by the U.S.-Japan Collaborative Program on Neutron Scattering. Work at Brookhaven National Laboratory was carried out under Contract No. DE-AC0276CH00016, Division of Material Science, U.S. Department of Energy.

[1]T. E. Mason, G. Aeppli, and H. A. Mook, Phys. Rev. Lett. **68**, 1414 (1992).
[2]M. Matsuda *et al.*, Phys. Rev. B **49**, 6958 (1994).
[3]J. Rossat-Mignod *et al.*, Physica B **163**, 4 (1990).
[4]J. M. Tranquada *et al.*, Phys. Rev. B **46**, 5561 (1992).
[5]This shifting of the spectral weight of $\chi''_{2d}(\omega)$ from low to high energies with doping, normalized to sample volume, has been demonstrated by Shamoto *et al.* (Ref. 18) in $YBa_2Cu_3O_{6+x}$ and by Matsuda *et al.* (Ref. 2) in $La_{2-x}Sr_xCuO_4$.
[6]R. J. Birgeneau *et al*, Phys. Rev. B **39**, 2868 (1989).
[7]S.-W. Cheong *et al.*, Phys. Rev. Lett. **67**, 1791 (1991).
[8]T. R. Thurston *et al.*, Phys. Rev. B **46**, 9128 (1992).
[9]B. J. Sternlieb *et al.*, Phys. Rev. B **47**, 5320 (1993).
[10]S. Shamoto, S. Hosoya, and M. Sato, Solid State Commun. **66**, 195 (1988).
[11]This sign choice optimizes the "focusing" of the spectrometer resolution function with respect to the $2d$ scattering.
[12]S. M. Hayden *et al.*, Phys. Rev. Lett. **66**, 821 (1991), a factored form for the dynamic susceptibility is also used in the analysis presented in this paper.
[13]A. J. Millis, H. Monien, and D. Pines, Phys. Rev. B **42**, 167 (1990).
[14]A. J. Millis and H. Monien, Phys. Rev. B **45**, 3059 (1992).
[15]V. Barzykin, D. Pines, A. Sokol, and D. Thelen, Phys. Rev. B **49**, 1544 (1994).
[16]D. Pines (private communication).
[17]V. J. Emery and S. A. Kivelson, Physica C **209**, 597 (1993).
[18]S. Shamoto *et al.*, Phys. Rev. B **48**, 13 817 (1993).